Solution Properties and Photonuclease Activity of Cationic Bis-porphyrins Linked with a Series of Aliphatic Diamines

Naoki YAMAKAWA, Yoshinobu ISHIKAWA, and Tadayuki UNO*

Faculty of Pharmaceutical Sciences, Kumamoto University, 5–1 Oe-honmachi, Kumamoto 862–0973, Japan.
Received June 18, 2001; accepted August 10, 2001

The development of efficient photo-induced DNA cleavage agents has been of particular interest for biomedical applications such as cancer photodynamic therapy (PDT). Toward this objective, we synthesized a series of cationic bis-porphyrins with various lengths of diamino alkyl linkage, *N*,*N*′-bis{4-[10,15,20-tris(1-methylpyridinium-4-yl)porphyrin-5-yl]benzoyl}oligomethylenediamine hexaiodide. They were expected to show more efficient photocleavage of DNA than unichromophore *meso*-tetrakis(4-*N*-methylpyridiniumyl)porphine (TMPyP), which is well known to cleave DNA effectively on illumination. The cationic bis-porphyrins were found to self-aggregate in aqueous solution, and the aggregation property was accounted for by the formation of an intermolecular dimer. Because conservative-type circular dichroism spectra of the bis-porphyrins were induced in the Soret region on binding to calf thymus DNA, we assigned their binding mode to outside self-stacking on the DNA surface. Their photonuclease activity using plasmid DNA decreased as the number of their linker hydrocarbons increased, and was well correlated with their tendency for dimerization. The inhibitory effect of azide anion, N_3^-, and the enhancement effect of D_2O suggest that singlet oxygen was probably involved in the photocleavage of DNA.

Key words porphyrin; DNA; photocleavage; aggregation; singlet oxygen

The development of photo-induced DNA cleavage agents is a progressive, growing field for biomedical applications such as cancer phototherapy.[1,2] In the application, selective cleavage of DNA in malignant cells can be achieved with DNA-specific photosensitizers by controlling the irradiation of light spatially. As a result of the DNA damage, the genetic events in the cells may be disturbed and thus the proliferation of tumor cells might be selectively suppressed. In order to cleave DNA effectively, both tight binding to DNA and efficient generation of active species responsible for the DNA damage are prerequisite for specific photosensitizers. Accordingly, it is very important to analyze in detail how the photosensitizers bind to and cleave DNA.

The interaction of DNA with cationic *meso*-tetrakis(4-*N*-methylpyridiniumyl)porphine (TMPyP) has been investigated because of its potential for both electrostatic binding to DNA and photonuclease activity.[3—5] For the binding, three major modes have been proposed: intercalation, outside binding in the groove, and outside binding with self-stacking along the DNA surface.[6] These binding modes have been suggested using the physicochemical method of viscometry[7,8] and spectroscopic techniques such as UV–visible absorption,[6—8] circular dichroism (CD),[6—9] fluorescence,[10,11] and NMR spectroscopy.[12,13] For the photonuclease activity, cationic TMPyP is more efficient in strand scission of plasmid DNA than an anionic porphyrin like hematoporphyrin derivative (HPD).[14,15] HPD is a complex mixture of oligo-porphyrins derived from hematoporphyrin,[16,17] and a purified fraction of HPD, Photofrin, is now clinically used in photodynamic therapy (PDT) of cancer.[18] Relationship between the binding mode and the photocleavage activity of TMPyP has also been pointed out.[15,19,20]

In addition to the bifunctionality of TMPyP, the cationic porphyrin is well taken up by HeLa cells and shows high phototoxicity, the extent of cellular damage being dependent on the light dose.[21] Furthermore, TMPyP is worth considering as a potential PDT candidate because of its excellent selectivity of tumor tissue and anti-tumor activity on photoexcitation, derived from studies *in vivo*.[22,23]

Although there have been extensive studies on unichromophore TMPyP with DNA, very few have been reported on the synthesis of cationic oligo-porphyrin and its interaction with DNA.[15] Such a molecule composed of two or more cationic porphyrin chromophores is expected to show higher efficiency of photocleavage of DNA than TMPyP, and hence to become a next-generation PDT candidate. In this paper, we report the synthesis of cationic bis-porphyrins **1**—**7**, which were linked with a series of aliphatic diamines, and the analyses of their solution properties, interaction with du-

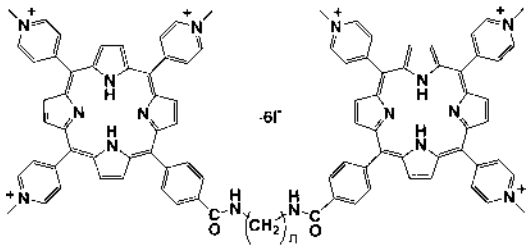

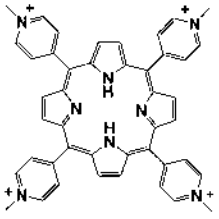

TMPyP

* To whom correspondence should be addressed. e-mail: unot@gpo.kumamoto-u.ac.jp

plex DNA, and photonuclease activity. We show that these cationic bis-porphyrins formed intermolecular dimers in aqueous solution, and bound to calf thymus DNA (CTDNA) with outside self-stacking. Their photocleavage efficiency of plasmid DNA diminished as the number of their linker hydrocarbons increased, and correlated with their tendency for dimerization.

Experimental

Instrumentation The ^{1}H-NMR spectra were recorded on a JEOL GX-400 or JNM-A-500 spectrometer. The MALDI-TOF (matrix-assisted laser desorption/ionization time-of-flight) mass spectra (MS) were measured on a Bruker REFLEX™. The UV–visible absorption measurement was performed on a Beckman DU650 spectrophotometer. The CD spectra were recorded on a JASCO J-720 spectropolarimeter. Elemental analyses were performed at the Analytical Center, Kumamoto University.

Materials and Methods Reagents for the synthesis of cationic bis-porphyrins were purchased from Tokyo Kasei Chemical Co. Thionyl chloride was distilled before use. Hexane, methylene chloride, and triethylamine were distilled in the presence of P_2O_5.[24] 5-(4-methoxycarbonylphenyl)-10,15,20-tris(4-pyridyl)porphine (TPyPCOOCH$_3$) and 5-(4-carboxyphenyl)-10,15,20-tris(4-pyridyl)porphine (TPyPCOOH) were synthesized according to the previous method.[25] CTDNA was purchased from Sigma Chemical Co., and the solution was quantitated spectrophotometrically using $\varepsilon_{260}=13200$ M (base pairs)$^{-1}\cdot$cm^{-1}. The tosylate salt of TMPyP was purchased from Dojin Chemical Co.

General Procedure for the Synthesis of Non-charged Bis-porphyrins Linked with a Series of Aliphatic Diamines TPyPCOOH (250 mg, 0.378 mmol) was dissolved in 35 ml of thionyl chloride under argon and the solution was refluxed for 2 h. After cooling to room temperature, thionyl chloride was removed under reduced pressure. Dry hexane (30 ml) was used to wash the residue and then removed. To this residue was added dry methylene chloride (40 ml), corresponding aliphatic diamine (0.4 eq to the mole of TPyPCOOH), and triethylamine (10 eq to the mole of TPyPCOOH) under argon. The reaction mixture was stirred for 20 h at room temperature. Chloroform, water, and a small amount of methanol were poured into the solution, and the organic phase was separated and dried with anhydrous Na_2SO_4. The solvent was removed and the corresponding bis-porphyrin was chromatographed on silica gel (2% methanol/$CHCl_3$) three times. Addition of heptane to the eluent and slow evaporation gave a brown powder, which was collected by centrifugation and dried.

N,*N*′-Bis[4-[10,15,20-tris(4-pyridyl)porphine-5-yl]benzoyl]ethylenediamine (**8**): Yield: 18% ^{1}H-NMR (10% $CD_3OD/CDCl_3$) δ: −2.91 (2H, s), 3.96 (4H, s), 8.17 (8H, d, J=6.3 Hz), 8.21 (4H, d, J=6.1 Hz), 8.35 (4H, d, J=8.5 Hz), 8.38 (4H, d, J=8.5 Hz), 8.85 (16H, m, br), 8.97 (8H, d, J=6.3 Hz), 9.02 (4H, d, J=6.1 Hz). UV λ_{max} (10% $CH_3OH/CHCl_3$) nm (ε): 644 (3650), 588 (9830), 547 (9590), 514 (32500), 418 (616000). MALDI-TOF-MS m/z: 1347.5 (M^+, Calcd for $C_{86}H_{58}N_{16}O_2$: 1347.5). *Anal.* Calcd for $C_{86}H_{58}N_{16}O_2\cdot 0.5H_2O\cdot 0.5CHCl_3\cdot 1C_7H_{16}$: C, 74.25; H, 4.75; N, 14.90. Found: C, 74.06; H, 5.02; N, 14.78.

N,*N*′-Bis[4-[10,15,20-tris(4-pyridyl)porphine-5-yl]benzoyl]trimethylenediamine (**9**): Yield: 20% ^{1}H-NMR (10% $CD_3OD/CDCl_3$) δ: −2.92 (2H, s), 2.17 (2H, m, br), 3.87 (4H, m, br), 8.08 (8H, d, J=6.5 Hz), 8.22 (4H, d, J=6.3 Hz), 8.35 (4H, d, J=8.3 Hz), 8.40 (4H, d, J=8.3 Hz), 8.83 (16H, m, br), 8.91 (8H, d, J=6.5 Hz), 9.03 (4H, d, J=6.3 Hz). UV λ_{max} (10% $CH_3OH/CHCl_3$) nm (ε): 645 (3510), 589 (7940), 547 (7690), 514 (26000), 418 (624000). MALDI-TOF-MS m/z: 1361.6 (M^+, Calcd for $C_{87}H_{60}N_{16}O_2$: 1361.5). *Anal.* Calcd for $C_{87}H_{60}N_{16}O_2\cdot 0.5H_2O\cdot 0.5CHCl_3\cdot 1C_7H_{16}$: C, 74.16; H, 5.10; N, 14.64. Found: C, 74.13; H, 4.96; N, 14.66.

N,*N*′-Bis[4-[10,15,20-tris(4-pyridyl)porphine-5-yl]benzoyl]tetramethylenediamine (**10**): Yield: 29% ^{1}H-NMR (10% $CD_3OD/CDCl_3$) δ: −2.92 (2H, s), 2.00 (4H, m, br), 3.76 (4H, m, br), 8.19 (8H, d, J=6.3 Hz), 8.21 (4H, d, J=6.1 Hz), 8.32 (8H, s, br), 8.86 (16H, m, br), 8.98 (8H, d, J=6.3 Hz), 9.02 (4H, d, J=6.1 Hz). UV λ_{max} (10% $CH_3OH/CHCl_3$) nm (ε): 645 (4760), 589 (10400), 547 (9980), 514 (34100), 418 (619000). MALDI-TOF-MS m/z: 1376.1 (M^+, Calcd for $C_{88}H_{62}N_{16}O_2$: 1375.6). *Anal.* Calcd for $C_{88}H_{62}N_{16}O_2\cdot 0.5H_2O\cdot 1CHCl_3\cdot 0.5C_7H_{16}$: C, 71.49; H, 4.67; N, 14.42. Found: C, 71.23; H, 4.87; N, 14.64.

N,*N*′-Bis[4-[10,15,20-tris(4-pyridyl)porphine-5-yl]benzoyl]pentamethylenediamine (**11**): Yield: 31% ^{1}H-NMR (10% $CD_3OD/CDCl_3$) δ: −2.97 (2H, s), 1.75 (2H, m, br), 1.95 (4H, m, br), 3.73 (4H, m, br), 7.94 (8H, d, J=5.4 Hz), 8.21 (4H, d, J=5.8 Hz), 8.31 (8H, s, br), 8.77 (16H, m, br), 8.81 (8H, d, J=5.4 Hz), 9.03 (4H, d, J=5.8 Hz). UV λ_{max} (10% $CH_3OH/CHCl_3$) nm (ε): 645 (4490), 589 (10300), 547 (10300), 514 (33400), 418 (613000). MALDI-TOF-MS m/z: 1390.2 (M^+, Calcd for $C_{89}H_{64}N_{16}O_2$: 1389.6). *Anal.* Calcd for $C_{89}H_{64}N_{16}O_2\cdot 0.5H_2O\cdot 1CHCl_3\cdot 0.5C_7H_{16}$: C, 71.21; H, 4.79; N, 14.21. Found: C, 71.55; H, 5.01; N, 14.32.

N,*N*′-Bis[4-[10,15,20-tris(4-pyridyl)porphine-5-yl]benzoyl]hexamethylenediamine (**12**): Yield: 52% ^{1}H-NMR (10% $CD_3OD/CDCl_3$) δ: −2.92 (2H, s), 1.70 (4H, m, br), 1.89 (4H, m, br), 3.69 (4H, m, br), 8.18 (8H, d, J=6.8 Hz), 8.21 (4H, d, J=5.8 Hz), 8.29 (4H, d, J=7.8 Hz), 8.32 (4H, d, J=7.8 Hz), 8.85 (16H, m, br), 8.98 (8H, d, J=6.8 Hz), 9.02 (4H, d, J=5.8 Hz). UV λ_{max} (10% $CH_3OH/CHCl_3$) nm (ε): 645 (4910), 590 (10400), 547 (9950), 515 (34500), 418 (619000). MALDI-TOF-MS m/z: 1404.3 (M^+, Calcd for $C_{90}H_{66}N_{16}O_2$: 1403.6). *Anal.* Calcd for $C_{90}H_{66}N_{16}O_2\cdot 1H_2O\cdot 1CHCl_3\cdot 0.5C_7H_{16}$: C, 71.34; H, 4.88; N, 14.08. Found: C, 71.31; H, 4.51; N, 13.89.

N,*N*′-Bis[4-[10,15,20-tris(4-pyridyl)porphine-5-yl]benzoyl]octamethylenediamine (**13**): Yield: 31% ^{1}H-NMR (10% $CD_3OD/CDCl_3$) δ: −2.92 (2H, s), 1.56 (8H, m, br), 1.84 (4H, m, br), 3.66 (4H, m, br), 8.18 (8H, d, J=6.1 Hz), 8.26 (4H, d, J=5.9 Hz), 8.24 (4H, d, J=7.5 Hz), 8.30 (4H, d, J=7.5 Hz), 8.86 (16H, m, br), 8.98 (8H, d, J=6.1 Hz), 9.02 (4H, d, J=5.9 Hz). UV λ_{max} (10% $CH_3OH/CHCl_3$) nm (ε): 645 (4700), 589 (10200), 547 (9770), 514 (33500), 418 (620000). MALDI-TOF-MS m/z: 1431.2 (M^+, Calcd for $C_{92}H_{70}N_{16}O_2$: 1431.7). *Anal.* Calcd for $C_{92}H_{70}N_{16}O_2\cdot 0.5H_2O\cdot 0.5CHCl_3\cdot 1C_7H_{16}$: C, 74.67; H, 5.51; N, 14.00. Found: C, 74.53; H, 5.29; N, 13.89.

N,*N*′-Bis[4-[10,15,20-tris(4-pyridyl)porphine-5-yl]benzoyl]decamethylenediamine (**14**): Yield: 25% ^{1}H-NMR (10% $CD_3OD/CDCl_3$) δ: −2.92 (2H, s), 1.46 (12H, m, br), 1.81 (4H, m, br), 3.64 (4H, m, br), 8.19 (8H, d, J=5.9 Hz), 8.21 (4H, d, J=6.1 Hz), 8.22 (4H, d, J=8.5 Hz), 8.29 (4H, d, J=8.5 Hz), 8.85 (16H, m, br), 8.99 (8H, d, J=5.9 Hz), 9.02 (4H, d, J=6.1 Hz). UV λ_{max} (10% $CH_3OH/CHCl_3$) nm (ε): 645 (4740), 589 (10300), 547 (9850), 514 (33800), 418 (622000). MALDI-TOF-MS m/z: 1459.2 (M^+, Calcd for $C_{94}H_{74}N_{16}O_2$: 1459.7). *Anal.* Calcd for $C_{94}H_{74}N_{16}O_2\cdot 0.5H_2O\cdot 0.5CHCl_3\cdot 1C_7H_{16}$: C, 74.86; H, 5.66; N, 13.76. Found: C, 75.12; H, 5.97; N, 14.09.

General Procedure for the Preparation of Cationic Bis-porphyrins Bis-porphyrins **8**—**14** (*ca*. 20 mg) were methylated in 15 ml of dimethylformamide (DMF) with methyl iodide (3 ml) for 3 h at room temperature. The solvent and methyl iodide were removed under vacuum. The residue was dissolved in DMF again and precipitated with diethyl ether. The brown powder was collected by centrifugation, washed with diethyl ether, and dried. This reaction was quantitative. Absorption spectra of **1**—**7** were measured in dimethyl sulfoxide (DMSO) and in the solution containing 10 mM sodium phosphate and 0.1 M sodium chloride (pH 7.0).

N,*N*′-Bis{4-[10,15,20-tris(1-methylpyridinium-4-yl)porphyrin-5-yl]-benzoyl}ethylenediamine Hexaiodide (**1**): ^{1}H-NMR (DMSO-d_6) δ: −3.02 (2H, s), 3.78 (4H, s), 4.72 (12H, s), 4.73 (6H, s), 8.39 (4H, d, J=7.5 Hz), 8.45 (4H, d, J=7.5 Hz), 9.01 (12H, d, J=6.8 Hz) 9.18 (16H, m, br), 9.48 (12H, d, J=6.8 Hz). UV λ_{max} (DMSO) nm (ε): 646 (13600), 591 (23500), 556 (23200), 514 (64700), 426 (565000); (buffer) nm (ε): 647 (4400), 589 (11000), 559 (10800), 523 (23900), 422 (311000). MALDI-TOF-MS m/z: 1438.3 (M^+, Calcd for $C_{92}H_{76}N_{16}O_2$: 1437.7). *Anal.* Calcd for $C_{92}H_{76}N_{16}O_2I_6\cdot 4H_2O\cdot 2DMF\cdot 0.5CH_3I$: C, 47.54; H, 4.03; N, 10.13. Found: C, 47.27; H, 4.18; N, 10.00.

N,*N*′-Bis{4-[10,15,20-tris(1-methylpyridinium-4-yl)porphyrin-5-yl]-benzoyl}trimethylenediamine Hexaiodide (**2**): ^{1}H-NMR (DMSO-d_6) δ: −3.02 (2H, s), 2.10 (4H, m, br), 3.66 (4H, m, br), 4.72 (12H, s), 4.73 (6H, s), 8.38 (4H, d, J=8.3 Hz), 8.43 (4H, d, J=8.3 Hz), 9.01 (12H, d, J=7.5 Hz) 9.18 (16H, m, br), 9.48 (12H, d, J=7.5 Hz). UV λ_{max} (DMSO) nm (ε): 646 (9240), 588 (20800), 555 (23300), 517 (45500), 426 (565000); (buffer) nm (ε): 650 (4480), 590 (10500), 562 (10700), 525 (22800), 421 (315000). MALDI-TOF-MS m/z: 1452.3 (M^+, Calcd for $C_{93}H_{78}N_{16}O_2$: 1451.8). *Anal.* Calcd for $C_{93}H_{78}N_{16}O_2I_6\cdot 6H_2O\cdot 1DMF\cdot 1CH_3I$: C, 46.05; H, 3.73; N, 9.25. Found: C, 45.94; H, 3.97; N, 9.39.

N,*N*′-Bis{4-[10,15,20-tris(1-methylpyridinium-4-yl)porphyrin-5-yl]-benzoyl}tetramethylenediamine Hexaiodide (**3**): ^{1}H-NMR (DMSO-d_6) δ: −3.02 (2H, s), 1.86 (4H, m, br), 3.58 (4H, m, br), 4.72 (12H, s), 4.73 (6H, s), 8.36 (4H, d, J=9.3 Hz), 8.41 (4H, d, J=9.3 Hz), 9.01 (12H, d, J=6.3 Hz) 9.17 (16H, m, br), 9.48 (12H, d, J=6.3 Hz). UV λ_{max} (DMSO) nm (ε): 646 (10100), 590 (20000), 556 (19200), 516 (50700), 425 (567000); (buffer) nm (ε): 650 (4370), 590 (10300), 562 (10700), 525 (21400), 421 (318000). MALDI-TOF-MS m/z: 1465.8 (M^+, Calcd for $C_{94}H_{80}N_{16}O_2$: 1465.8). *Anal.* Calcd for $C_{94}H_{80}N_{16}O_2I_6\cdot 4H_2O\cdot 0.5DMF\cdot 1CH_3I$: C, 46.78; H, 3.84; N, 9.33. Found: C, 47.10; H, 3.76; N, 9.01.

N,*N*′-Bis{4-[10,15,20-tris(1-methylpyridinium-4-yl)porphyrin-5-yl]-

benzoyl}pentamethylenediamine Hexaiodide (**4**): ^{1}H-NMR (DMSO-d_6) δ: −3.02 (2H, s), 1.62 (2H, m, br), 1.82 (4H, m, br), 3.53 (4H, m, br), 4.72 (12H, s), 4.73 (6H, s), 8.35 (4H, d, J=8.3 Hz), 8.40 (4H, d, J=8.3 Hz), 9.01 (12H, d, J=7.0 Hz), 9.17 (16H, m, br), 9.48 (12H, d, J=7.0 Hz). UV λ_{max} (DMSO) nm (ε): 645 (10200), 590 (20100), 556 (20000), 516 (53700), 425 (565000); (buffer) nm (ε): 651 (4620), 591 (9860), 562 (10700), 526 (19900), 419 (313000). MALDI-TOF-MS *m/z*: 1480.1 (M^+, Calcd for $C_{95}H_{82}N_{16}O_2$: 1479.8). *Anal.* Calcd for $C_{95}H_{82}N_{16}O_2I_6\cdot 6H_2O\cdot 1DMF\cdot 1CH_3I$: C, 46.27; H, 3.99; N, 9.15. Found: C, 46.37; H, 4.09; N, 9.29.

N,*N*′-Bis{4-[10,15,20-tris(1-methylpyridinium-4-yl)porphyrin-5-yl]-benzoyl}hexamethylenediamine Hexaiodide (**5**): ^{1}H-NMR (DMSO-d_6) δ: −3.03 (2H, s), 1.58 (4H, m, br), 1.77 (4H, m, br), 3.51 (4H, m, br), 4.72 (12H, s), 4.73 (6H, s), 8.35 (4H, d, J=7.3 Hz), 8.38 (4H, d, J=7.3 Hz), 9.01 (12H, d, J=6.3 Hz), 9.17 (16H, m, br), 9.48 (12H, d, J=6.3 Hz). UV λ_{max} (DMSO) nm (ε): 646 (11300), 590 (21100), 556 (20400), 515 (53600), 426 (566000); (buffer) nm (ε): 651 (4600), 591 (9690), 562 (10400), 526 (19600), 418 (317000). MALDI-TOF-MS *m/z*: 1493.9 (M^+, Calcd for $C_{96}H_{84}N_{16}O_2$: 1493.8). *Anal.* Calcd for $C_{96}H_{84}N_{16}O_2I_6\cdot 6H_2O\cdot 1DMF\cdot 1CH_3I$: C, 46.58; H, 4.14; N, 9.24. Found: C, 46.25; H, 3.91; N, 9.40.

N,*N*′-Bis{4-[10,15,20-tris(1-methylpyridinium-4-yl)porphyrin-5-yl]-benzoyl}octamethylenediamine Hexaiodide (**6**): ^{1}H-NMR (DMSO-d_6) δ: −3.03 (2H, s), 1.49 (8H, m, br), 1.73 (4H, m, br), 3.46 (4H, m, br), 4.72 (12H, s), 4.73 (6H, s), 8.30 (4H, d, J=7.3 Hz), 8.37 (4H, d, J=7.3 Hz), 9.01 (12H, d, J=7.0 Hz), 9.17 (16H, m, br), 9.48 (12H, d, J=7.0 Hz). UV λ_{max} (DMSO) nm (ε): 646 (9520), 590 (19600), 556 (18900), 517 (48000), 425 (561000); (buffer) nm (ε): 651 (4180), 591 (10100), 561 (10800), 524 (21000), 417 (312000). MALDI-TOF-MS *m/z*: 1521.1 (M^+, Calcd for $C_{98}H_{88}N_{16}O_2$: 1521.9). *Anal.* Calcd for $C_{98}H_{88}N_{16}O_2I_6\cdot 6H_2O\cdot 1DMF\cdot 0.5CH_3I$: C, 47.72; H, 4.31; N, 9.44. Found: C, 48.08; H, 4.31; N, 9.39.

N,*N*′-Bis{4-[10,15,20-tris(1-methylpyridinium-4-yl)porphyrin-5-yl]-benzoyl}decamethylenediamine Hexaiodide (**7**): ^{1}H-NMR (DMSO-d_6) δ: −3.03 (2H, s), 1.42 (12H, m, br), 1.71 (4H, m, br), 3.45 (4H, m, br), 4.72 (12H, s), 4.73 (6H, s), 8.33 (4H, d, J=9.3 Hz), 8.36 (4H, d, J=9.3 Hz), 9.01 (12H, d, J=7.3 Hz), 9.17 (16H, m, br), 9.48 (12H, d, J=7.3 Hz). UV λ_{max} (DMSO) nm (ε): 645 (9930), 590 (19100), 556 (18200), 516 (50100), 425 (558000); (buffer) nm (ε): 648 (4010), 590 (10500), 559 (10600), 523 (23400), 419 (313000). MALDI-TOF-MS *m/z*: 1549.9 (M^+, Calcd for $C_{100}H_{92}N_{16}O_2$: 1549.9). *Anal.* Calcd for $C_{100}H_{92}N_{16}O_2I_6\cdot 6H_2O\cdot 2DMF\cdot 0.5CH_3I$: C, 48.52; H, 4.57; N, 9.56. Found: C, 48.64; H, 4.68; N, 9.64.

Spectral Measurements Aliquots of CTDNA solution were added to the solution of a cationic bis-porphyrin (*ca.* 4.0 μM). Spectral measurements were performed at 25 °C in the buffer containing 10 mM sodium phosphate and 100 mM sodium chloride (pH 7.0). The binding constant (K) and the number of binding sites per base pair (n) were estimated from the spectral changes, following Scatchard analysis.[26—29]

DNA Photocleavage Assay Photoirradiation was performed at 25 °C using a HITACHI 650-60 fluorescence spectrophotometer. A sample containing supercoiled pUC18 plasmid DNA and a cationic bis-porphyrin was irradiated in a buffer (10 mM sodium phosphate and 0.1 M NaCl, pH 7.0) at 432 nm for 30 min. After irradiation, DNA was analyzed by agarose gel (0.8%) electrophoresis at 100 V. The gel was incubated in a solution of ethidium bromide and the DNA bands were detected by fluorescence under a UV lamp. The densitometric data of the bands were obtained with an ATTO Densitograph version 4.0 for Macintosh. The staining intensity of relaxed plasmid DNA was found to be 1.5 times that of supercoiled DNA.[30] The results were corrected based on this difference.

Results

Synthesis of Cationic Bis-porphyrins Linked with a Series of Aliphatic Diamines The synthetic procedures for the non-charged bis-porphyrins **8**—**14** and the cationic bis-porphyrins **1**—**7** are illustrated in Chart 1. We used TPyPCOOH as a framework for the synthesis of the "dumbbell-like" porphyrins. TPyPCOOH was readily obtained by alkali hydrolysis of $TPyPCOOCH_3$, which was synthesized by the mixed-aldehyde method using 1 eq of terephthalaldehydic acid methyl ester, 3 eq of pyridine-4-aldehyde, and 4 eq of pyrrole in propionic acid.[25] On direct coupling of 1 eq of TPyPCOOH with 0.5 eq of ethylenediamine, 1,3-diaminopropane, 1,4-diaminobutane, 1,5-diaminopentane, 1,6-diaminohexane, 1,8-diaminooctane, or 1,10-diaminodecane, the use of carbonyldiimidazole or *N*,*N*′-dicyclohexylcarbodiimide as a coupling reagent did not give the desired compounds. Alternatively, the direct coupling by way of acid chlorination of TPyPCOOH allowed us to obtain a series of bis-porphyrins, **8** (Yield: 18%), **9** (20%), **10** (29%), **11** (31%), **12** (52%), **13** (31%), and **14** (25%). The non-charged bis-porphyrins were then methylated with methyl iodide in DMF for 3 h to give the final products **1**—**7** quantitatively. All these cationic bis-porphyrins could be dissolved in 10 mM phosphate buffer (pH 7.0) and their stock solutions (150 μM) were used for the experiments mentioned below.

Characteristics of Cationic Bis-porphyrins in Aqueous Solution. Absorption spectra of **1**—**7** and TMPyP were recorded in DMSO and in the solution containing 10 mM sodium phosphate and 0.1 M sodium chloride (pH 7.0). The cationic bis-porphyrins showed an intense absorption band, called the Soret band, at 400—450 nm. The extinction coefficients ($\varepsilon^{Soret}_{buffer}$ and $\varepsilon^{Soret}_{DMSO}$) of the Soret maximum ($\lambda^{Soret}_{max}$) for **1**—**7** in the buffer and DMSO are listed in Table 1, and a significant solvent effect was apparent: the $\varepsilon^{Soret}_{DMSO}$ of **1**—**7** was commonly 1.8 times larger than the $\varepsilon^{Soret}_{buffer}$ of them. In addition, the $\varepsilon^{Soret}_{buffer}$ of the cationic bis-porphyrins was only 1.3 times as large as $\varepsilon^{Soret}_{buffer}$ of unichromophore TMPyP, whereas the $\varepsilon^{Soret}_{DMSO}$ was 1.9 times larger than $\varepsilon^{Soret}_{DMSO}$ of TMPyP, approaching the expected value.

This solvent effect was examined in detail using absorption spectrometry. Figure 1 shows the extinction coefficient development at λ^{Soret}_{max} in the buffered solutions of TMPyP, **1**, **5**, and **7** with addition of DMSO. Only a slight increase of the ε was observed for TMPyP, whereas large hyperchromicity was seen for the cationic bis-porphyrins. In particular, the ε of **7** doubled in the presence of 70% DMSO (v/v).

The $\varepsilon^{Soret}_{buffer}$ of **1**—**7** decreased with increase in their concentrations from 0.2 to 90 μM, as shown typically in Fig. 2a for **1**. This hypochromicity was well accounted for by the formation of an intermolecular dimer. The dimerization constant can be obtained from Eq. 1[31,32]:

$$[(\varepsilon_M-\varepsilon_{obs})/C_M]^{1/2}=(2K_D/\Delta\varepsilon)^{1/2}[\Delta\varepsilon-(\varepsilon_M-\varepsilon_{obs})] \quad (1)$$

where ε_{obs}, ε_M, and ε_D are the extinction coefficients of the solution, the pure monomer, and the pure dimer, respectively, C_M is the concentration based on the molecular weight of the monomer unit, $\Delta\varepsilon$ is $\varepsilon_M-\varepsilon_D$, and K_D is the equilibrium constant of dimerization. A plot of $[(\varepsilon_M-\varepsilon_{obs})/C_M]^{1/2}$ *vs.* $(\varepsilon_M-\varepsilon_{obs})$ yields a straight line (Fig. 2b) from which the value of K_D for **1**—**7** was obtained (Table 1). It is clear that their K_D values were larger as their linkers lengthened.

Titration of Cationic Bis-porphyrins with Duplex DNA: Visible Spectroscopy Complexation between a ligand molecule and DNA leads to absorption spectral changes that can be used to monitor the binding process. The extraordinarily large extinction coefficient of the Soret band for the cationic bis-porphyrins allowed spectrophotometric detection of porphyrin–DNA interactions at very low concentrations (4—5 μM). The solutions of TMPyP and the cationic bis-porphyrins were titrated with a stock solution of CTDNA, which contains 42% of GC base pairs, in a buffer (10 mM sodium phosphate and 0.1 M NaCl, pH 7.0). For TMPyP, the intensity of the Soret band decreased monotonously with one set of isosbestic points as shown in Fig. 3a. Furthermore, the λ^{Soret}_{max} shifted to longer wavelength (bathochromic shift:

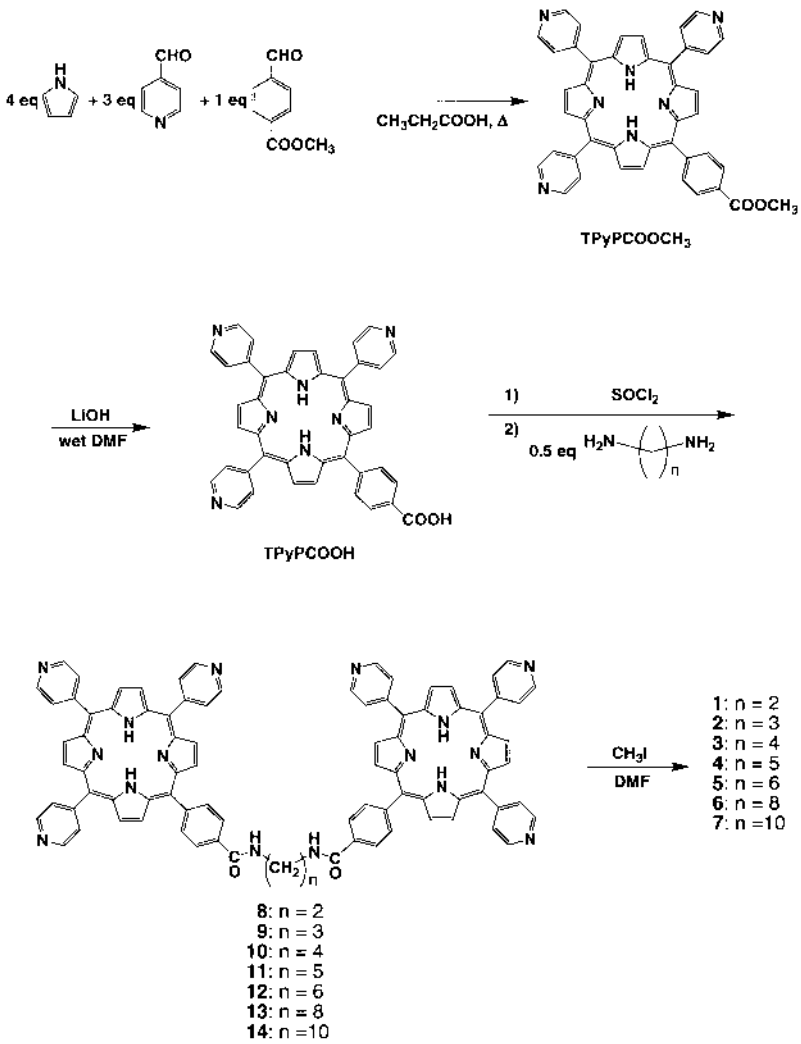

Chart 1

Table 1. The Extinction Coefficients of λ_{max}^{Soret} for **1**—**7** in the Buffer[a] and DMSO, and Their Dimerization Constants

	TMPyP	**1**	**2**	**3**	**4**	**5**	**6**	**7**
$\varepsilon_{buffer}^{Soret}\times10^{-3}$ ($M^{-1}\cdot cm^{-1}$)	243	311	315	318	313	317	312	313
$\varepsilon_{DMSO}^{Soret}\times10^{-3}$ ($M^{-1}\cdot cm^{-1}$)	295	565	565	567	565	566	561	558
$K_D\times10^{-3}$ (M^{-1})		19	21	30	31	33	34	38

a) 10 mM sodium phosphate and 0.1 M NaCl (pH 7.0).

$\Delta\lambda = 10$ nm) and showed large hypochromicity (46%). The hypochromicity was determined by the equation $H = (A_f - A_b)/(A_f)\times100$, where A_f and A_b represent the Soret absorbances of free and bound porphyrins, respectively. Because of the presence of the isosbestic points throughout the titration, the optical contribution certainly came from two distinct species, free and bound porphyrin chromophore. Thus, the binding constant (K) and the number of binding sites per base pair (n) could be estimated by the Scatchard analysis. The values of K and n were estimated to be 4.3 μM^{-1} and 0.34, respectively. A theoretical curve with these values nicely reproduced the absorbance change of the Soret maximum as shown in Fig. 3b.

Contrary to the monotonous spectral change of TMPyP, the spectral behavior of the cationic bis-porphyrins with addition of CTDNA was complex. The intensity of the λ_{max}^{Soret} of each bis-porphyrin decreased together with a red shift at the initial step, and then the intensity of the red shifted peak increased with further DNA additions. The spectral change for **2** titrated with CTDNA is shown in Fig. 4a. No characteristic isosbestic point was observed in any case of the bis-porphyrins. Figure 4b shows the absorbance change at the λ_{max}^{Soret} of **2**. Clearly, the binding process for **2** was more than two steps, and other bis-porphyrins also showed similar behavior. While the bathochromic shift of the cationic bis-porphyrins ($\Delta\lambda = 9$—15 nm) was close to that of TMPyP, their hypochromicity (2—13%) was smaller than that of TMPyP (Table 2).

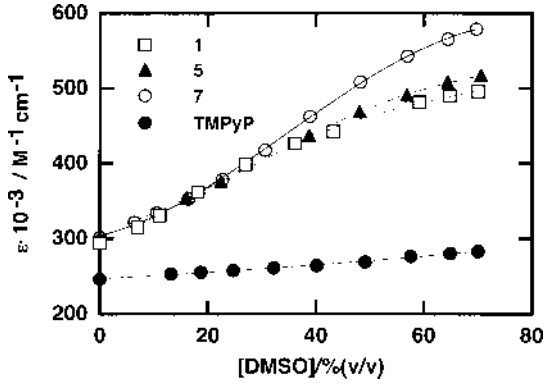

Fig. 1. Extinction Coefficient Development at λ_{max}^{Soret} in the Buffered Solution (10 mM Sodium Phosphate and 0.1 M NaCl, pH 7.0) of **1** (Open Squares), **5** (Filled Triangles), **7** (Open Circles), and TMPyP (Filled Circles) with Addition of DMSO

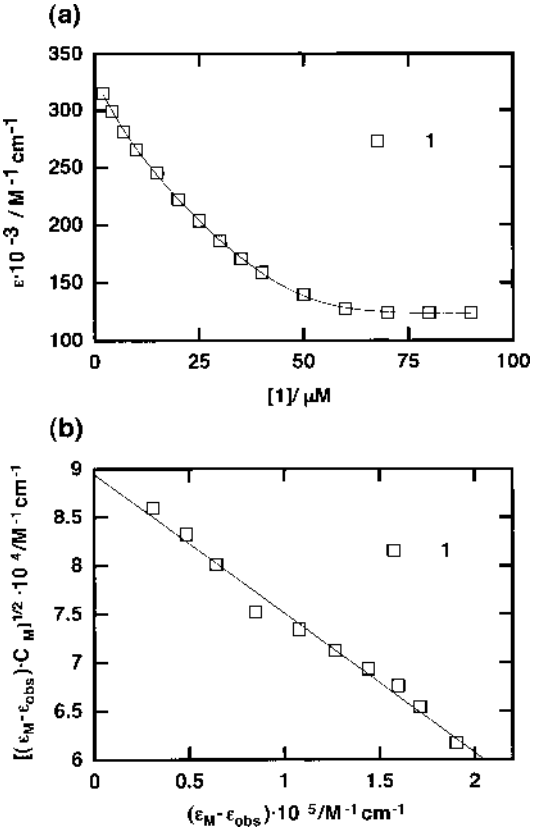

Fig. 2. (a) Extinction Coefficient Change at λ_{max}^{Soret} in the Buffered Solution (10 mM Sodium Phosphate and 0.1 M NaCl, pH 7.0) of **1** with Increase in Its Concentration; (b) Plot to Determine the Dimerization Constant of **1** Using the λ_{max}^{Soret} in the Buffered Solution.

Concentrations ranged from 0.27 μM to 90 μM

Induced CD in the Soret Region CD is a powerful spectroscopic technique that has been widely used to trace conformational changes of DNA and to study the interaction with external ligands.[33,34] CD spectra generally show positive and/or negative bands, and hence are more sensitive and informative than absorption spectra.[29] In addition, induced circular dichroism (ICD) in the Soret region, especially the sign of ICD spectrum, is very helpful for analysis of the binding mode of an achiral porphyrin to chiral DNA.[3,4,6]

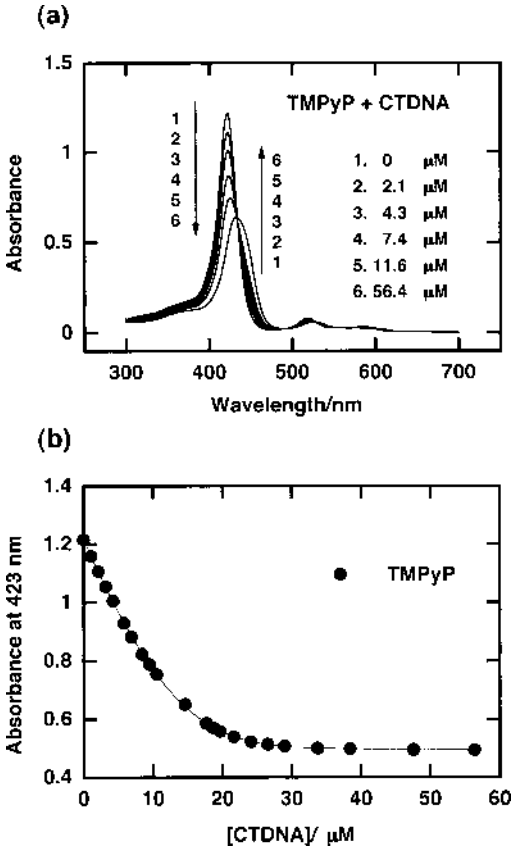

Fig. 3. (a) Absorption Spectral Change of TMPyP (5.3 μM) with Addition of CTDNA in the Buffered Solution Containing 10 mM Sodium Phosphate and 0.1 M NaCl (pH 7.0); (b) Absorbance Change of TMPyP at 423 nm with Addition of CTDNA

The cationic porphyrins, TMPyP and **1**—**7**, did not show any ICD in the absence of duplex DNA, but characteristic spectra in the Soret region were induced with addition of DNA in a buffer (10 mM sodium phosphate, pH 7.0). Figure 5a shows the ICD spectra of TMPyP bound to CTDNA at various salt (NaCl) concentrations at $R=0.01$, where R denotes input ratio of [porphyrin]/[base pairs]. In the presence of 0.1 M NaCl the ICD spectrum comprised both a large negative peak at 437 nm and a relatively small positive peak at 417 nm. However, the ellipticity of the negative peak developed and that of the positive peak decreased as the salt concentration decreased. In the absence of NaCl the positive band was lost and a dominant large negative band was observed. In the case of bis-porphyrins, both positive and negative peaks were also clear in the presence of 0.1 M NaCl, as shown in Fig. 5b for **1** at $R=0.01$. The large positive peak at 417 nm decreased and the negative peak at 437 nm developed as the salt concentration decreased. Unlike the case of TMPyP, however, the ICD spectrum of **1** in the absence of NaCl remained conservative with almost equivalent ellipticities.

Photocleavage of Plasmid DNA The photonuclease activity for **1**—**7** was examined using supercoiled double-stranded pUC18 plasmid DNA. A mixture of the cationic porphyrin (0.48 μM, $R=0.008$) and the plasmid DNA (60 μM) in a buffer (10 mM sodium phosphate and 0.1 M NaCl, pH 7.0) was irradiated in air at 432 nm for 30 min. After irradiation, conversion of the supercoiled DNA (form I) to nicked

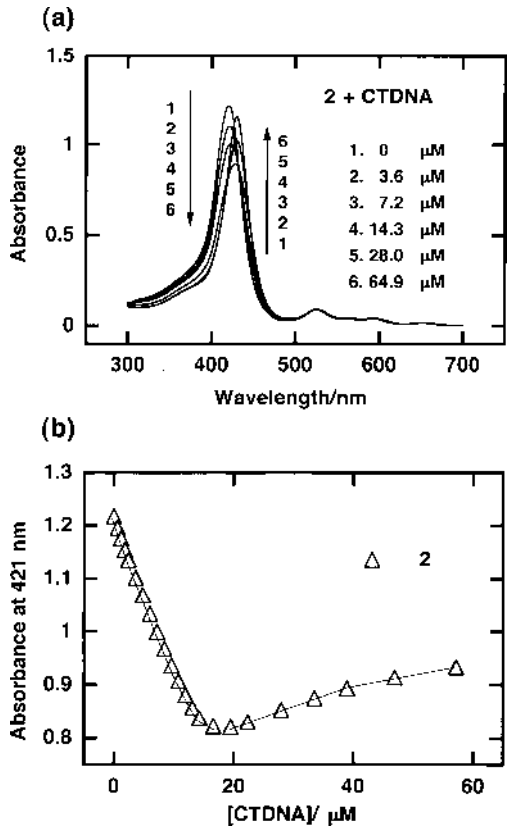

Fig. 4. (a) Absorption Spectral Change of **2** (3.8 μM) with Addition of CTDNA in the Buffered Solution Containing 10 mM Sodium Phosphate and 0.1 M NaCl (pH 7.0); (b) Absorbance Change of **2** at 421 nm with Addition of CTDNA

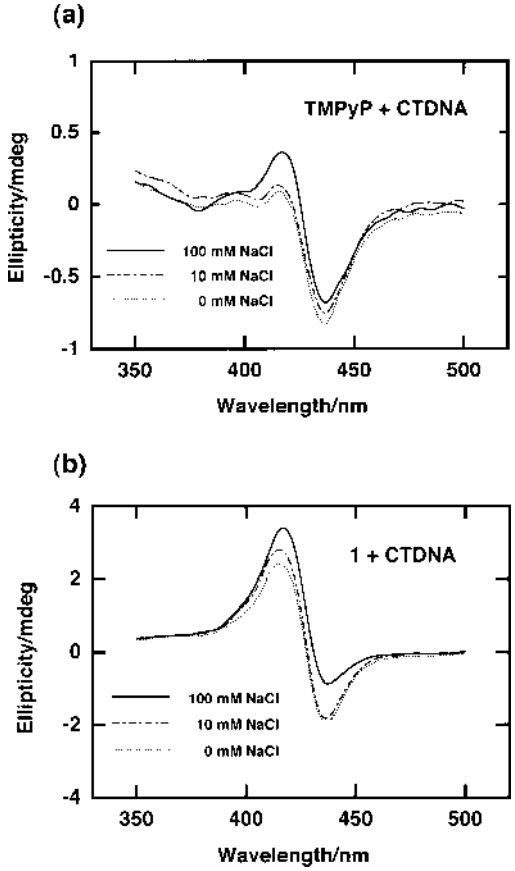

Fig. 5. (a) ICD Spectra of TMPyP (3.8 μM) in the Presence of CTDNA (382 μM) at Various NaCl Concentrations; (b) ICD Spectra of **1** (3.8 μM) in the Presence of CTDNA (382 μM) at Various NaCl Concentrations

Table 2. Spectroscopic Data for TMPyP and **1**—**7** Bound to CTDNA in the Buffer[a)]

	TMPyP	**1**	**2**	**3**	**4**	**5**	**6**	**7**
$\Delta\lambda$ (nm)	10	9	11	11	13	13	15	13
H (%)	46	2	6	8	9	10	11	13

a) 10 mM sodium phosphate and 0.1 M NaCl (pH 7.0).

circular DNA (form II) was visualized by agarose gel electrophoresis with ethidium bromide staining. On generation of a single-strand break, form I is converted to form II, which migrates more slowly on the gel than form I. Figure 6 shows the percentage of form II DNA, obtained from the densitometric analysis of the gel electrophoresis. In this reaction condition, TMPyP (form II: 45%) and **1** (44%) showed almost the same degrees of conversion of form I to form II, while **2** (34%), **3** (28%), **4** (24%), **5** (21%), **6** (16%), and **7** (7%) exhibited a lower degree of conversion than TMPyP. The photonuclease activity of these cationic bis-porhyrins was lower as their linkers lengthened. As shown in Fig. 7, **1**, **4**, and **7** caused a linear increase of form II DNA as irradiation time increased. Their conversion rates at R=0.01 ([porphyrin]=0.6 μM) were 2.1%/min for **1**, 1.6%/min for **4**, 1.1%/min for **7**, and 1.8%/min for TMPyP, and hence lower as the number of their linker hydrocarbons increased.

The influence of DMSO on the photocleavage activity was examined. DMSO is well known as a hydroxyl radical scavenger,[35)] and was also a polar solvent that increased the ε of

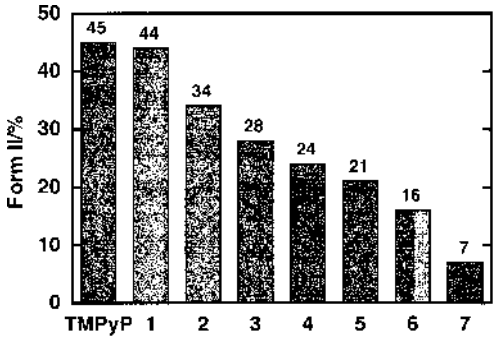

Fig. 6. Percentages of Form II DNA Obtained from the Densitometric Data of the Result of Gel Electrophoresis after pUC18 Plasmid DNA (60 μM) Were Treated with TMPyP and **1**—**7** (0.48 μM) in the Presence of Light (432 nm) and Air for 30 min at 25 °C in the Buffered Solution Containing 10 mM Sodium Phosphate and 0.1 M NaCl (pH 7.0)

λ_{max}^{Soret} of the cationic bis-porphyrins in the buffer, as mentioned above. As shown in Fig. 8, the increase of DMSO concentration (0 to 30%, v/v) in the buffer resulted in increase of form II DNA in the presence of **7** on illumination.

Electrostatic binding of **7** to DNA was confirmed by monitoring the extent of strand scission with increasing amount of NaCl in the reaction mixture. As shown in Fig. 9, increase in the concentration of NaCl resulted in a continuous reduction of form II DNA during 30 min of illumination, and almost complete protection was seen with 300 mM NaCl.

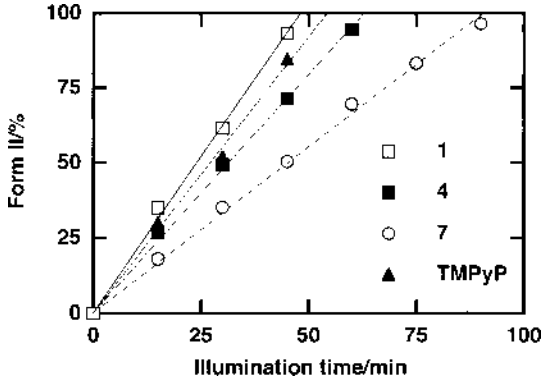

Fig. 7. Influence of the Illumination Time on the Formation of Form II DNA Induced by **1** (Open Squares), **4** (Filled Squares), **7** (Open Circles), and TMPyP (Filled Triangles)

Cleavage conditions: 0.6 μM **1**, **4**, **7**, and TMPyP; 60 μM pUC18 plasmid DNA; 10 mM sodium phosphate and 0.1 M NaCl (pH 7.0); irradiation at 432 nm for 30 min at 25 °C.

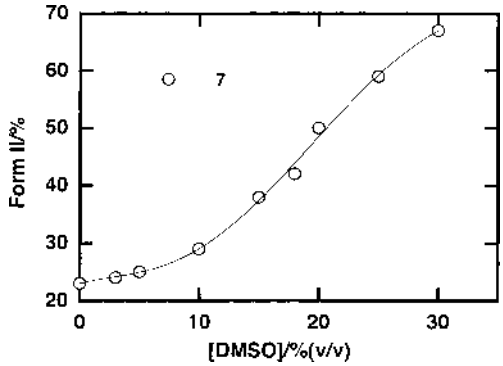

Fig. 8. Influence of DMSO Concentrations (v/v) on the Formation of Form II DNA Photoinduced by **7**

Cleavage conditions: 0.6 μM 7; 60 μM pUC18 plasmid DNA; 10 mM sodium phosphate and 0.1 M NaCl (pH 7.0); irradiation at 432 nm for 30 min at 25 °C.

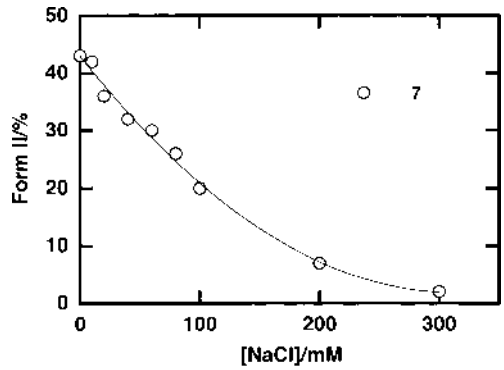

Fig. 9. Inhibitory Effect of NaCl on the Formation of Form II DNA Photoinduced by **7**

Cleavage conditions: 0.6 μM 7; 60 μM pUC18 plasmid DNA; 10 mM sodium phosphate and 0.1 M NaCl (pH 7.0); irradiation at 432 nm for 30 min at 25 °C.

In order to identify the active species responsible for the photonuclease activity, NaN_3, an excellent $^1O_2$ quencher,[36] was added instead of NaCl in the reaction mixture. The activity of **7** was significantly inhibited in the presence of NaN_3 (Fig. 10a). Clearly, the concentration of NaN_3 (*ca.* 20 mM) required for 50% inhibition of the activity was lower than that of NaCl (*ca.* 90 mM). If $^1O_2$ was generated in this system, one would expect that the photonuclease activity would be enhanced by replacing the reaction media of H_2O by D_2O, which makes the lifetime of $^1O_2$ longer.[37] The replacement actually increased the activity of **7**, as shown in Fig. 10b.

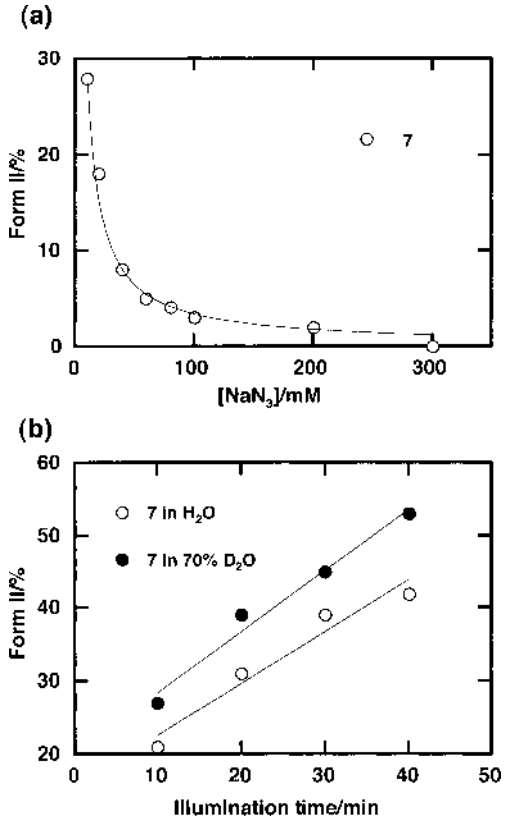

Fig. 10. (a) Inhibitory Effect of NaN_3 on the Formation of Form II DNA Photoinduced by **7**; (b) Influence of Reaction Media of H_2O (Open Circles) and 70% D_2O (Filled Circles) on the Formation of Form II DNA Photoinduced by **7**

Cleavage conditions: 0.6 μM 7; 60 μM pUC18 plasmid DNA; 10 mM sodium phosphate and 0.1 M NaCl (pH 7.0); irradiation at 432 nm for 30 min at 25 °C.

Discussion

The objective of our research was to synthesize a series of cationic bis-porphyrins with various lengths of diamino alkyl linkage, and to analyze both their binding to duplex DNA and photonuclease activity. Cationic unichromophore TMPyP has the characteristics of high quantum yield for the formation of singlet oxygen ($^1O_2$),[38] strong affinity with DNA,[7] and much more efficient photonuclease activity than anionic porphyrins and HPD.[14,15] Thus, we anticipated that these bis-porphyrins containing two TMPyP-like chromophores in a molecule might exhibit more enhanced photonuclease activity than TMPyP.

Synthesis As the framework for the synthesis of bis-porphyrins, we adopted asymmetrical porphyrin TPyPCOOH bearing three 4-pyridyl groups and one 4-carboxyphenyl group at the peripheral position (Chart 1). To know the linker effect of the cationic bis-porphyrins on their solution properties and functions, a series of saturated aliphatic diamines with different numbers of hydrocarbons ($-C_nH_{2n}-$, $n=2$ to 10) was chosen. Bis-porphyrins bridged through the amide bond were also expected to be stable against their decomposition in aqueous solution. Hence, the conjugation between

1 eq of TPyPCOOH and 0.5 eq of a corresponding aliphatic diamine was accomplished by direct coupling *via* acid chlorination of TPyPCOOH to give the dumbbell-like porphyrins **8**—**14** with modest yield (18—52%). Finally, the quaternization of six 4-pyridyl groups in the non-charged bis-porphyrins using methyl iodide gave **1**—**7** quantitatively.

Solution Properties Some kinds of cationic porphyrins tend to aggregate spontaneously in aqueous solution,[39,40] and the propensity is known to influence the interaction between cationic porphyrins and DNA.[8,41—44] Therefore, the characterization in the solution state of these cationic bis-porphyrins was first done by visible spectrometry. The value of the $\varepsilon^{\text{Soret}}_{\text{buffer}}$ of **1**—**7** (*ca.* $3.1\times10^5\,\text{M}^{-1}\cdot\text{cm}^{-1}$) was markedly different from that of their $\varepsilon^{\text{Soret}}_{\text{DMSO}}$ (*ca.* $5.6\times10^5\,\text{M}^{-1}\cdot\text{cm}^{-1}$). In addition, the $\varepsilon^{\text{Soret}}_{\text{buffer}}$ of **1**—**7** was 1.3 times as large as that of unichromophore TMPyP ($2.43\times10^5\,\text{M}^{-1}\cdot\text{cm}^{-1}$), whereas their $\varepsilon^{\text{Soret}}_{\text{DMSO}}$ was 1.9 times larger than that of TMPyP ($2.95\times10^5\,\text{M}^{-1}\cdot\text{cm}^{-1}$). These large differences in the extinction coefficients between the buffer and DMSO should be attributed to self-aggregation of porphyrin chromophores in aqueous solution. The extinction coefficient changes with addition of DMSO to the buffered solution of **1**, **5**, and **7** were monitored, and large hyperchromicity was observed for these bis-porphyrins (Fig. 1). This hyperchromicity was probably due to the relaxation of the self-aggregation by solvation of DMSO around the π-surfaces of porphyrin chromophores interacting with each other in the buffer.[39,45]

The aggregation property was examined by varying the concentration of **1**—**7** ranging from 0.2 to 90 μM in the buffered solution. The $\varepsilon^{\text{Soret}}_{\text{buffer}}$ of **1**, for instance, decreased from 3.13×10^5 to $1.23\times10^5\,\text{M}^{-1}\cdot\text{cm}^{-1}$ with increase in the concentrations (Fig. 2a), and other cationic bis-porphyrins showed similar behavior. This hypochromicity with increase in the concentrations indicates the occurrence of intermolecular interaction of bis-porphyrins, but not intramolecular interaction between two porphyrin chromophores in a bis-porphyrin molecule. We presumed that the solution behavior of **1**—**7** was based on a simple monomer–dimer equilibrium, and the dimerization constant K_D of **1**—**7** could be estimated using Eq. 1. The good fitness of a theoretical line shown for **1** (Fig. 2b) and others clearly shows that they dimerized in aqueous solution within the concentration range examined, though TMPyP is known not to aggregate at concentrations lower than 10^{-3} M.[46] Because the value of K_D for **1**—**7** increased as the linkers lengthened (Table 1), hydrophobicity of the linker parts in the cationic bis-porphyrins must be responsible for the stability of their intermolecular aggregation state.

DNA Binding With increasing concentration of the natural DNA, the intensity of $\lambda^{\text{Soret}}_{\text{max}}$ of TMPyP decreased monotonously with one set of isosbestic points in the buffered condition (Fig. 3a). The spectral change was accompanied by a bathochromic shift (10 nm) and large hypochromicity (46%). The substantial hypochromicity seems to be a sign of the intercalative binding mode.[6] The binding process was found to be in a single step by the Scatchard analysis (Fig. 3b), and the n estimated (0.34) is indicative of the binding of a TMPyP molecule per three base pairs to CTDNA. On the other hand, the binding process of **2** (Figs. 4a and b) and other cationic bis-porphyrins with addition of CTDNA was more than two steps without any characteristic isosbestic points, and thus we were unable to obtain their binding parameters due to their binding complexity. The complicated binding process for **1**—**7** may be derived from perturbation of their aggregation states. Their moderate hypochromicity (2—13%) was much smaller than that of TMPyP, and hence their binding mode to CTDNA seems not to be intercalation.

The conservative asymmetric ICD spectrum of TMPyP–CTDNA complex at $R=0.01$ in the presence of 0.1 M NaCl changed to a single negative spectrum in the absence of NaCl (Fig. 5a). This ICD spectral change exhibits the ionic strength dependence of the binding of TMPyP to CTDNA.[47] The transition of the binding would be from mixed or outside self-stacking to intercalative mode. Because the relative viscosity of CTDNA with addition of TMPyP in the presence of 0.1 M NaCl increased (data not shown), TMPyP must be actually intercalated.[48,49] In contrast to TMPyP, the conservative asymmetric ICD signal of **1** in the presence of 0.1 M NaCl became more symmetric in the absence of NaCl (Fig. 5b). On the basis of their conservative ICD spectra and solution properties mentioned above, the cationic bis-porphyrins clearly bound to CTDNA with outside self-stacking.

Photocleavage The photonuclease activity of **1**—**7** using pUC18 plasmid DNA and electrophoretic technique at $R=0.008$ for 30 min illumination was well correlated with their alkyl linker lengths (Fig. 6). The photocleavage of DNA at $R=0.01$ for **1**, **4**, and **7** was linearly dependent on illumination time, and **1** (2.1%/min) was about twice as efficient as **7** (1.1%/min) in the photocleavage (Fig. 7). Comparison with the conversion rate (1.8%/min) for TMPyP showed that these bis-porphyrins containing two TMPyP-like chromophores in a molecule, which were linked with a series of aliphatic diamines, did not show full photonuclease activity as we expected. The fact that the bis-porphyrins linked with longer alkyl linkage showed less photonuclease activity corresponded with their self-aggregation properties. Because their dimerization constants were larger as their linkers lengthened, their dimer components were not likely to be involved in their photonuclease activity. As a result, it may not be suitable to use aliphatic diamines as the linker in designing bis-porphyrins showing the desired photonuclease activity.

It is well known that photosensitization of dyes promotes DNA strand breaks *via* three main pathways: hydroxyl radical attack, electron transfer process (type I mechanism), or oxidation by singlet oxygen (energy transfer process, type II).[50] The addition of DMSO, known to hydroxyl radical scavenger, in our system increased the photonuclease activity of **7** (Fig. 8). This enhanced activity implies that the active species would not be diffusible hydroxyl radical.[51] The enhancement should be related to the relaxation of the aggregation state and/or the higher producibility for active species. The exclusion of diffusible hydroxyl radical as the active species in the system was supported by reduction of the activity with increase in amount of NaCl (Fig. 9). This result could be explained by the electrostatic and tight binding of Na^+ to phosphate diester backbone of DNA to prevent access of the cationic bis-porphyrins and certain active species to the vicinity of DNA. The active species in our system did not seem to be diffusible.

The addition of NaN_3 to the system significantly inhibited the photonuclease activity (Fig. 10a). Because the $^1O_2$ quencher (IC_{50} *ca.* 20 mM) inhibited the activity more effi-

ciently than NaCl (IC_{50} *ca.* 90 mM), the inhibitory effect should be derived from quenching of short-lived $^1O_2$, generated from the photoactivated bis-porphyrin and $^3O_2$, in the presence of N_3^-, in addition to prevention of the porphyrin binding to DNA in the presence of Na^+. Moreover, the involvement of $^1O_2$ in the photocleavage was evidenced from the enhancement of the activity by replacing the reaction media of H_2O by D_2O (Fig. 10b). The aggregation state of the cationic bis-porphyrins in aqueous solution would influence their production of $^1O_2$.[52]

Comparison with Cationic Porphyrin–Acridine Hybrids We have recently reported the synthesis of cationic porphyrin–acridine hybrids, their interaction with DNA, and photonuclease activity.[25] The ICD data on their binding to CTDNA suggested that the acridine part and TMPyP-like unit in the hybrids interacted with the DNA by intercalative and outside groove binding, respectively. In addition, the length of their diamino alkyl linkage was found to influence markedly the ellipticity of their positive ICD in the Soret region. These data suggested that the proximity of the TMPyP-like unit in the hybrids to the exterior of CTDNA was greatly affected by their linker lengths. On the other hand, the present study showed that the bis-porphyrins containing two TMPyP-like units bound to CTDNA with outside self-stacking on the DNA surface; this was shown by their conservative-type ICD in the Soret region. Thus, the TMPyP-like unit changes its binding mode according to the property of the appendant. Although both TMPyP and acridine can bind to CTDNA through intercalation, there was no sign for intercalation of the TMPyP-like unit in the bis-porphyrins. Consequently, the cationic porphyrin unit is unlikely to serve as an appropriate intercalator in designing conjugated DNA-interactive agents.

The cationic porphyrin–acridine hybrids also exhibited more efficient photocleavage of plasmid DNA than TMPyP, while the cationic bis-porphyrins did not show the expected photonuclease activity. The fact that TMPyP-like unit in the hybrids lay in the groove in binding to CTDNA suggested the cationic unit is a monomer state, whereas the cationic one in the bis-porphyrins seemed to self-aggregate on the DNA surface. It is likely that the aggregation of the TMPyP-like unit in the conjugates in binding to DNA varies its producibility of reactive oxygen species, such as $^1O_2$, generated on illumination, and thus influences their photonuclease activity considerably.

In conclusion, we synthesized cationic bis-porphyrins linked with a series of aliphatic diamines, and found them to form an intermolecular dimer in aqueous solution. These cationic bis-porphyrins did not have expected photonuclease activity, and their intermolecular dimers did not seem to be responsible for the activity. The development of cationic bis-porphyrins capable of showing fully enhanced photonuclease activity is in progress in our laboratory.

Acknowledgments This research was supported in part by a Grant-in-Aid to T. U. for Scientific Research from the Ministry of Education, Science, Sports, Culture and Technology of Japan (grant no. 11470476).

References and Notes

1) Amitage B., *Chem. Rev.*, **98**, 1171—1200 (1998).
2) Ali H., van Lier J. E., *Chem. Rev.*, **99**, 2379—2450 (1999).
3) Fiel R. J., *J. Biomol. Struc. Dyn.*, **6**, 1259—1274 (1989).
4) Pasternack R. F., Gibbs E. J., *Met. Ions Biol. Syst.*, **33**, 367—397 (1996).
5) Marzilli L. G., *New. J. Chem.*, **14**, 409—420 (1990).
6) Pasternack R. F., Gibbs E. J., Villafranca J. J., *Biochemistry*, **22**, 2406—2414 (1983).
7) Fiel R. J., Howard J. C., Mark E. H., Datta Gupta N., *Nucleic Acids Res.*, **6**, 3093—3118 (1979).
8) Carvlin M. J., Fiel R. J., *Nucleic Acids Res.*, **11**, 6121—6139 (1983).
9) Carvlin M. J., Mark E. H., Fiel R. J., *Nucleic Acids Res.*, **11**, 6141—6154 (1983).
10) Sari M. A., Battioni J. P., Dupre D., Mansuy D., Le Pecq J. B., *Biochemistry*, **29**, 4205—4215 (1990).
11) Sehlstedt U., Kim S. K., Carter P., Goodisman J., Vollano J. F., Norden B., Dabrowiak J. C., *Biochemistry*, **33**, 417—426 (1994).
12) Marzilli L. G., Banville D. L., Zon G., Wilson W. D., *J. Am. Chem. Soc.*, **108**, 4188—4192 (1986).
13) Guliaev A. B., Leontis N. B., *Biochemistry*, **38**, 15425—15437 (1999).
14) Fiel R. J., Datta-Gupta N., Mark E. H., Howard J. C., *Cancer Res.*, **41**, 3543—3545 (1981).
15) Praseuth D., Gaudemer A., Verlhac J.-B., Kraljic I., Sissoeff I., Guille E., *Photochem. Photobiol.*, **44**, 717—724 (1986).
16) Lipson R. L., Baldes E. J., *Arch. Dermatol.*, **82**, 508—516 (1960).
17) Dougherty T. J., Lawrence G., Kaufman J. H., Bovle D., Weishaupt K. R., *J. Natl. Cancer Inst.*, **62**, 231—237 (1979).
18) Dougherty T. J., *Photochem. Photobiol.*, **58**, 895—900 (1993).
19) Croke D. T., Perrouault L., Sari M. A., Battioni J.-P., Mansuy D., Helene C., Le Doan T., *J. Photochem. Photobiol. B*, **18**, 41—50 (1993).
20) Nussbaum J. M., Newport M. E. A., Mackie M., Leontis N. B., *Photochem. Photobiol.*, **59**, 515—528 (1994).
21) Villanueva A., Juarranz A., Diaz V., Gomez J., Canete M., *Anti-Cancer Drug Des.*, **7**, 297—303 (1992).
22) Villanueva A., Jori G., *Cancer Lett.*, **73**, 59—64 (1993).
23) Villanueva A., Caggiari L., Jori G., Milanesi C., *J. Photochem. Photobiol. B*, **23**, 49—56 (1994).
24) Armarego W. L. F., Perrin D. D., "Purification of Laboratory Chemicals, Fourth Edition," Butterworth-Heinemann, Oxford, 1996.
25) Ishikawa Y., Yamashita A., Uno T., *Chem. Pharm. Bull.*, **49**, 287—293 (2001).
26) Scatchard G., *Ann. N.Y. Acad. Sci.*, **51**, 660—672 (1949).
27) McGhee J. D., von Hippel P. H., *J. Mol. Biol.*, **86**, 469—489 (1974).
28) Correia J. J., Chaires J. B., *Methods Enzymol.*, **240**, 593—614 (1994).
29) Uno T., Hamasaki K., Tanigawa M., Shimabayashi S., *Inorg. Chem.*, **36**, 1676—1683 (1997).
30) Nielsen P. E., Jeppesen C., Egholm M., Buchardt O., *Biochemistry*, **27**, 6338—6343 (1988).
31) Schwartz G. Klose S. Balthasar W., *Eur. J. Biochem.*, **12**, 454—460 (1970).
32) Jennette K. W. Gill J. T. Sadownick J. A. Lippard S. J., *J. Am. Chem. Soc.*, **98**, 6159—6168 (1976).
33) Rodger A., Norden B., "Circular Dichroism and Linear Dichroism," Oxford Chemistry Masters, Oxford University Press, Oxford, New York, Tokyo, 1997.
34) Zimmer C., Luck G., "Advances in DNA Sequence Specific Agents," Vol. 1, ed. by Hurley L. H., JAI Press Inc., Greenwich, 1992, pp. 51—88.
35) Repine J. E., Pfenninger O. W., Talmage D. W., Berger E. M., Pettijhon D. E., *Proc. Natl. Acad. Sci. U.S.A.*, **78**, 1001—1003 (1981).
36) Foote C. S., Fujimoto T. T., Chang Y. C., *Tetrahedron Lett.*, **1972**, 45—48.
37) Kajiwara T., Kearns D. R., *J. Am. Chem. Soc.*, **95**, 5886—5890 (1973).
38) Verlhac J. B., Gaudemer A., Kraljic I., *Nouv. J. Chim.*, **8**, 401—406 (1984).
39) Jin R., Aoki S., Shima K., *J. Chem. Soc.*, *Faraday Trans.*, **1997**, 3945—3953.
40) Kano K., Fukuda K., Wakami H., Nishiyabu R., Pasternack R. F., *J. Am. Chem. Soc.*, **122**, 7494—7502 (2000).
41) Carlvin M. J., Datta-Gupta N., Fiel R. J., *Biochem. Biophys. Res. Commun.*, **108**, 66—73 (1982).
42) Mukundan N. E., Petho G., Dixon D. W., Kim M. S., Marzilli L. G., *Inorg. Chem.*, **33**, 4676—4687 (1994).
43) Mukundan N. E., Petho G., Dixon D. W., Marzilli L. G., *Inorg. Chem.*, **34**, 3677—3687 (1995).
44) Dixon D. W., Steullet V., *J. Inorg. Biochem.*, **69**, 25—32 (1998).
45) Karaman R., Bruice T. C., *J. Org. Chem.*, **56**, 3470—3472 (1991).
46) Vergeldt F. J., Koehorst R. B. M., van Hoek A., Schaafsma T. J., *J.*

Phys. Chem., **99**, 4397—4405 (1995).
47) Pasternack R. F., Garrity P., Ehrlich B., Davis C. B., Gibbs E. J., Orloff G., Giartosio A., Turano C., *Nucleic Acids Res*., **14**, 5919—5931 (1986).
48) Banville D. L., Margilli L. G., Wilson W. D., *Biochem. Biophys. Res. Commun*., **113**, 148—154 (1983).
49) Tjahjono D. H., Akutsu T., Yoshioka N., Inoue H., *Biochim. Biophys. Acta*, **1472**, 333—343 (1999).
50) Paillous N., Vicendo P., *J. Photochem. Photobiol. B*, **20**, 203—209 (1993).
51) Ishikawa Y., Morishita Y., Yamamoto T., Kurosaki H., Goto M., Matsuo H., Sugiyama M., *Chem. Lett.*, **1998**, 39—40.
52) Ricchelli F., *J. Photochem. Photobiol. B*, **29**, 109—118 (1995).